ACS APPLIED MATERIALS & INTERFACES

Research Article

www.acsami.org

Biodegradation and Toxicity of Protease/Redox/pH Stimuli-Responsive PEGlated PMAA Nanohydrogels for Targeting Drug delivery

Sha Jin,[†] Jiaxun Wan,[†] Lizheng Meng,[§] Xiaoxing Huang,[§] Jia Guo,[†] Li Liu,[§] and Changchun Wang*[,†]

[†]State Key Laboratory of Molecular Engineering of Polymers, and Department of Macromolecular Science, Laboratory of Advanced Materials, Fudan University, Shanghai 200433, China

[§]Shanghai Institute of Phamaceutical Industry, Shanghai 200000, China

Supporting Information

ABSTRACT: The application of nanomaterials in intelligent drug delivery is developing rapidly for treatment of cancers. In this paper, we fabricated a new kind of protease/redox/pH stimuli-responsive biodegradable nanohydrogels with methacrylic acid (MAA) as the monomer and *N*,*N*-bis(acryloyl)-cystamine (BACy) as the cross-linker through a facile reflux-precipitation polymerization. After that, the polyethylene glycol (PEG) and folic acid (FA) were covalently grafted onto the surface of the nanohydrogels for enhancement of their long in vivo circulation lifetime and active targeting ability to the tumor cells and tissues. This kind of nanohydrogels could be disassembled into short polymer chains (M_n < 1140; PDI < 1.35) both in response to glutathione (GSH) through reduction of the sensitive disulfide bonds and protease by breakage of the amido bonds in the cross-linked networks. The nanohydrogels were utilized to simultaneously load both hydrophilic drug doxorubicin (DOX) and hydrophobic drug paclitaxel (PTX) with high drug loading efficiency. The cumulative release profile showed that the drug release from the drug-loaded nanohydrogels was significantly expedited by weak acidic (pH 5.0) and reducing environment (GSH), which exhibited an distinct redox/pH dual stimuli-responsive drug release to reduce the leakage of drugs before they reach tumor site. In addition, the in vitro experiment results indicated that the multidrug-loaded system had synergistic effect on cancer therapy. Meanwhile, the acute toxicity and intravital fluorescence imaging studies were adopted to evaluate the biocompatibility and biotoxicity of the nanohydrogels, the experimental results showed that the PEG modification could greatly enhance the long in vivo circulation lifetime and reduce the acute toxicity (LD_{50}: from 138.4 mg/kg to 499.7 mg/kg) of the nanohydrogels.

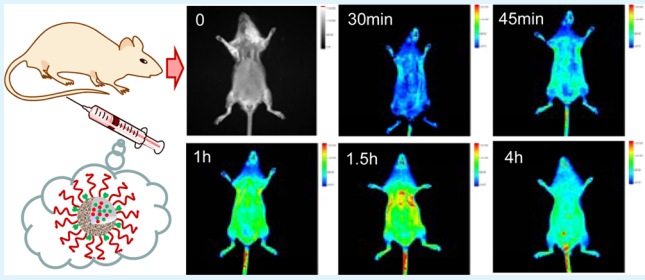

KEYWORDS: *nanohydrogels, surface modification, dual-drug loading, multi stimuli-responsive, biodegradable, acute toxicity, intravital fluorescence imaging*

1. INTRODUCTION

Chemotherapy in treatment of cancers was controversial for a long time due to the systemically delivery and unpleasant side effects.[1−3] To achieve better control over the drug concentration, residence time, activity in harsh conditions, and administration frequency, the researchers inclined to adopt intelligent carriers for targeted drug delivery.[4] Among the numerous developed drug carriers, the multifunctional nanohydrogels provide a soft microenvironment similar to that of the tissue and a diminished surface tension to biological systems, along with tunable physicochemical characteristics and low cytotoxicity, which give a great potential for targeted drug delivery.[5−8]

To date, the efficient targeting of drug carriers usually involves two aspects. One is the passive targeting via enhanced permeability and retention effect (EPR), in which a detachable poly(ethylene glycol) (PEG) protective layer is often utilized to prevent nanohydrogels from being captured by the reticuloendothelial system (RES) and nonspecific attack by macrophages to increase the blood circulation lifetime.[9−11] Another is the active targeting via targeted ligands for overexpressed receptors on the surface of the cells.[12] Folate has been demonstrated as an effectively targeted molecule to the overexpressed folate-receptor tumor cells, endowing the drug carriers with the advantage of high binding affinity.[13−15]

Administration of hydrophobic anticancer drugs, such as paclitaxel (PTX) and camptothecin, has faced a big challenge in cancer therapy because of their low drug efficiency originated from their low water solubility.[16,17] And it is also difficult for hydrophilic nanogel carriers to load such drugs because of the lack of strong interactions. However, we found that the hydrophobic domains introduced in nanohydrogels could form

Received: July 3, 2015
Accepted: August 19, 2015
Published: August 19, 2015

DOI: 10.1021/acsami.5b05984
ACS Appl. Mater. Interfaces 2015, 7, 19843−19852

hydrophobic interactions with the hydrophobic drugs, thus greatly increasing the drug loading efficency.[18−21] Just as we thought, if the drugs with different anticancer mechanisms will work at different growth stages of tumor cells, then loading of multiple drugs in one drug carrier can act synergistically to gain superior response and patient survival rate.[22,23] Tumor cells usually have a unique environment including lower pH and higher redox potential compared with normal cells, which can be exploited as stimuli triggers for responsive drug release.[24−28] Nanohydrogels with carboxyl groups can change their ionic states according to intracorporal pH, and thus can control the releasing of the electrostatic binding drugs.[29−31]

Generally, the kidney can excrete compounds smaller than 50 kDa, so a biocompatible polymer that can biodegrade to small oligomers is very important for the metabolism in human body.[32−34] The disulfide-cross-linked nanohydrogels can be rapidly dissociated by the glutathione (GSH) in tumor cells and promote the release of noncovalent encapsulated drugs.[35,36] Besides, if the cross-linked agent we adopted has amido bonds in the polymer chains, it can be broken by abundant proteases or lipases in the body, implying the potential of the degradability of the drug carrier in normal tissue or organs.

Despite recent burgeoning developments, preparation of advanced nanohyrogels with delicate structures and novel properties are still confronted with great challenges. On the basis of our previous work,[37,38] we herein fabricated a series of uniform biodegradable nanohydrogels (disulfide cross-linked PMAA) through a facile reflux-precipitation polymerization (RPP), which were then conjugated with PEG and folate, respectively, using the carbodiimide coupling method to endow the nanocarriers with long in vivo circulation lifetime and folate receptor-mediated endocytosis. On the basis of this deliberate design, the nanohydrogels possessed high loading capacity for both hydrophilic and hydrophobic drugs, and achieved quick responses to pH/GSH stimuli for controlled drug release. Moreover, protease-mediated degradation experiments indicated their great potential of metabolic ability in normal tissue and organs. In addition, the acute toxicity studies and intravital fluorescence imaging were adopted to evaluate the biotoxicity and biodistribution of the nanohydrogels.

2. EXPERIMENTAL SECTION

2.1. Materials. Methacrylic acid (MAA), acrylic acid (AA), and *N*,*N*-methylene bis(acrylamide) (MBA) were purchased from Sigma-Aldrich. 2,2-Azobis(isobutyronitrile) (AIBN) was supplied by Sinopharm Chemical Reagent Company and recrystallized before use. Acryloyl chloride, ethylene diamine, *N*,*N*′-dicyclohexylcarbodiimide (DCC), *N*-(3-(dimethylamino)propyl)-*N*′-ethylcarbodiimide hydrochloride (EDC·HCl), *N*-hydroxy succinimide (NHS), glutathione (GSH), protease K and folic acid were purchased from Shanghai Aladdin Chemistry Co. Ltd. PEG-NH_2 (M_w = 1000) was supplied by Huntsman Corporation. Cystamine dihydrochloride was obtained from Acros. Doxorubicin (DOX), in the form of a hydrochloride salt, and paclitaxel (PTX) were purchased from Beijing Huafeng United Technology Company. Acetonitrile (AN) and methanol were purchased from Shanghai Lingfeng Chemical Reagent Company. Acetone was purchased from Shanghai Dahe Chemical Reagent Company. Dichloromethane, dimethyl sulfoxide (DMSO), ethyl acetate, and heptane were obtained from Shanghai Chemical Reagents Company. Deionized water was used in all our experiments.

2.2. Animals. The ICR mice used in the acute toxicity study and in vivo distribution study were purchased from shanghai laboratory animal center. Mice were housed in a room with ad libitum access to food and water under a 12 h light/dark cycle. All experiments were approved by the local Ethics Committee for the use of experimental animals and complied with the Guidelines for the Care and Use of Laboratory Animals.

2.3. Synthesis of Disulfide Cross-Linker of *N*,*N*-Bis(acryloyl)-cystamine (BACy). In this part, the *N*,*N*-Bis(acryloyl)cystamine was synthesized through the reaction of cystamine dihydrochloride with acryloyl chloride in dichloromethane. More details of the fabrication process for this cross-linker were reported earlier.[38,39]

2.4. Preparation of PMAA Nanohydrogels. Utilizing reflux-precipitation polymerization, we prepared the PMAA nanohydrogels in this section. The detailed procedure was described earlier.[38]

2.5. Amination of Folic Acid (FA-NH_2). The preparation of FA-NH_2 was carried out according to method described in ref 40.

2.6. Preparation of Folate-Conjugated PMAA (FA-PMAA) Nanohydrogels. In this section, the folate-conjugated PMAA (FA-PMAA) nanohydrogels was prepared according to the method described in a published paper.[8]

2.7. Preparation of PEGlated FA-PMAA [(PEG&FA)-PMAA] Nanohydrogels. The PEG-NH_2 (M_w = 1000) was conjugated to FA-PMAA nanohydrogels using the carbodiimide coupling method. Typically, FA-PMAA nanohydrogels (30 mg) was dispersed in acetonitrile (20 mL). After addition of 48 mg EDC·HCl and 28.75 mg NHS, the mixture was heated to 70 °C and stirred for another 3 h. 60 mg PEG-NH_2 was then added, and the reaction mixture was stirred overnight at 70 °C. The obtained (PEG&FA)-PMAA nanohydrogels were separated and purified by repeating ultracentrifugation (12 000 rpm for 3 min)/decantation/resuspension (in acetonitrile with ultrasonic bathing) for three times. The purified nanohydrogels were dried overnight under vacuum at 45 °C.

2.8. Redox-Triggered Disassembly of (PEG&FA)-PMAA Nanohydrogels. The disassembly of the (PEG&FA)-PMAA nanohydrogels responded to reducing agents (GSH) was monitored by the turbidity of the dispersion according to ref 38. Besides, the molecular weight of the degraded polymers was measured by gel permeation chromatography (GPC).

2.9. Protease-Mediated Disassembly of (PEG&FA)-PMAA Nanohydrogels. The turbidity change of the (PEG&FA)-PMAA dispersion responded to protease K was monitored by dynamic light scattering (DLS) measurement according to published paper.[38] Different from that in ref 38, the reducing agent GSH was replaced with protease K.

2.10. Acute Toxicity Study. The acute toxicity studies were carried out on ICR mice weighing 20−22 g. A total of 50 mice (for one kind of nanohydrogels) were randomly divided into five groups, 10 mice per group and 5 mice for each sex. The mice were fasted overnight but had free access to water. The dispersed suspension of nanohydrogels was injected through caudal vein at grade doses. The general behavior, toxic symptoms and mortality were observed at 1, 2, 4 h after dosing, and then further observed once a day up to 14 days for behavioral changes and signs of toxicity and/or death. The body weights were monitored on day 0, 3, 7, and 14, and their food intaken was monitored on days 0, 3, and 12. At the end of the study, all the surviving animals were euthanized and then the organs were removed for necropsy. Finally, the median lethal dose (LD_{50}) was calculated on the basis of animal death at different dose levels.

2.11. Intravital Fluorescence Imaging. In vivo real-time fluorescence imaging analysis was used to evaluate the in vivo distribution of the prepared nanohydrogels. The ICR mouse was anesthetized using sodium pentobarbital (25 mg/kg, i.p.). The dispersed suspension of FITC-labeled nanohydrogels was injected through caudal vein at a dose of 200 μL (1 mg/mL of FITC). The mouse was placed on an animal plate heated to 37 °C. The fluorescent images were captured at various time points using the Optical and X-ray small animal imaging system (Bruker, excitation: 410−760 nm, emission: 535−830 nm).

2.12. Drug Loading Capacity in (PEG&FA)-PMAA Nanohydrogels. Loading of PTX: Typically, 10 mg of dry (PEG&FA)-PMAA nanohydrogels and 2 mg of PTX were dispersed in 3 mL of acetone under stirring at room temperature. After 2/3 volume of acetone was evaporated, the dispersion was then centrifugated to collect the sediments of PTX-loaded (PEG&FA)-PMAA nanohydrogel

DOI: 10.1021/acsami.5b05984
ACS Appl. Mater. Interfaces 2015, 7, 19843−19852

Scheme 1. Preparation of FA- and PEG-Modified PMAA Nanohydrogels for Multi-Drug Loading and Releasing

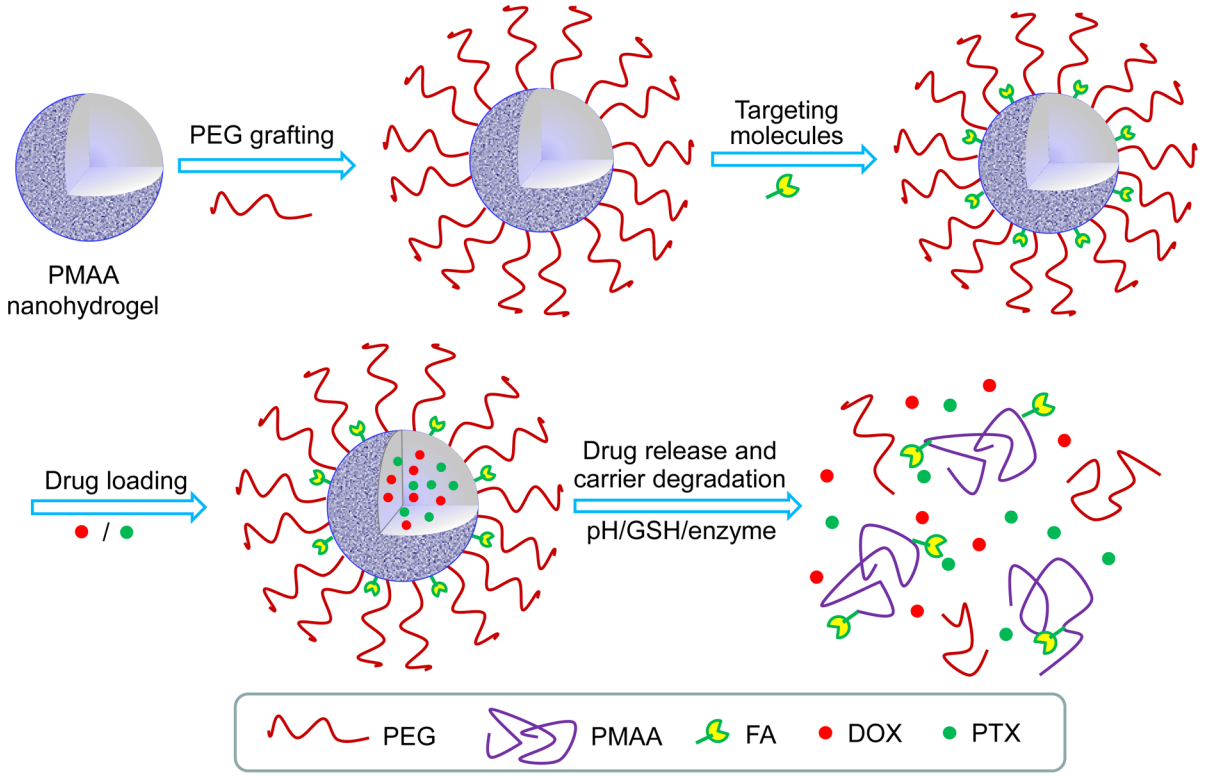

and washed with water for three times to remove the unloaded and surface adsorbed PTX. The purified drug-loaded nanohydrogels were freeze-dried. The PTX mass loaded in nanohydrogels was calculated by a UV−visible spectrophotometer at 228 nm (comparing with PTX calibration curve) after extracting PTX from the dried drug-loaded nanohydrogels with methanol. Loading of DOX: the DOX loading procedure was same as the published paper.[8]

The drug loading content (DLC) and drug loading efficiency (DLE) were calculated according the following equations:

$$\text{DLC (\%, PTX)} = \frac{\text{weight of PTX in methanol}}{\text{weight of drug loaded nanohydrogel}} 100\%$$

$$\text{DLC (\%, DOX)} = \frac{\text{initial weight of DOX} - \text{weight of DOX in supernatant}}{\text{weight of drug loaded nanohydrogel}} 100\%$$

$$\text{DLE (\%)} = \frac{\text{weight of DOX or PTX in nanohydrogel}}{\text{initial weight of DOX or PTX}} 100\%$$

2.13. In Vitro Release of Drugs from (PEG&FA)-PMAA nanohydrogels. In this section, the drug release of the drug-loaded (PEG&FA)-PMAA nanohydrogels in vitro was measured according to ref 38.

2.14. Confocal laser Scanning Microscopy (CLSM) Observation. The cellular uptake of the dual-drug-loaded (PEG&FA)-PMAA was confirmed by confocal laser scanning microscopy (CLSM) observation. Typically, the HeLa cells were seeded in 6-well culture plates (a clean coverslip was put in each well) and grown overnight, then the cells were incubated with dual-drug-loaded (PEG&FA)-PMAA at 37 °C for 24 h. At 2h, 6h, and 24h, the cells were rinsed with PBS for three times, fixed with 2.5% formaldehyde (1 mL per well) at 37 °C for 10 min, and then rinsed with PBS three times again. To perform nucleus labeling, the nuclei was stained with 4,6-diamidino-2-phenylindole (DAPI) solution (20 mg mL^{-1} in PBS, 1 mL per well) for 10 min and then rinsed with PBS three times. The coverslips were placed on a glass microscope slide, and the samples were visualized using CLSM (Olympus, FV10-ASW).

2.15. In Vitro Cell Assays. The cytotoxicity assay was performed by cell counting kit-8 (CCK-8) assay.[41] The detailed procedure was same as in ref 38.

2.16. Characterization. All the measurement methods were same as in ref 38.

2. RESULTS AND DISCUSSION

3.1. Synthesis and Characterization of PMAA Nanohydrogels. The synthesis route of the nanohydrogels was illustrated in Scheme 1. First, the PMAA nanohydrogels cross-linked by disulfide cross-linker BACy were fabricated through the facile reflux-precipitation polymerization (RPP).[42] Then, the FA-NH_2 and amino-terminated PEG was grafted onto the surface of the nanohydrogels by adopting the carbodiimide coupling reaction, respectively. After that, the PEG and folate conjugated nanohydrogels were loaded with PTX and DOX step by step. Because of the sensitive response to pH and GSH triggers, the loaded drugs can be quickly released from the nanohydrogles in targeting sites and kill the tumor cells when they enter the tumorous tissues. After that, the nanohydrogels also can be biodegraded into short polymer chains in human body by GSH and protease.

To prepare a nanohydrogel with a suitable morphology and size, we conducted a series of experiments with different reaction parameters. Through shortening the reaction time of reflux-precipitation polymerization, we obtained nanohydrogels with relative small sizes suitable for in vivo transportation. The typical recipes and tested results were listed in Table 1. From Table 1, we found that the particle sizes of nanohydrogels increased from 147 to 285 nm on TEM and from 437 to 620 nm on DLS as the ratio of the disulfide cross-linker increased (MB1-MB4), the polydispersity index (PDI) of DLS was

DOI: 10.1021/acsami.5b05984
ACS Appl. Mater. Interfaces 2015, 7, 19843−19852

Table 1. Recipes and Characterization of the PMAA Nanohydrogels with Different Cross-linker Contents

sample code	MAA (mg)	BACy (mg)	D_{TEM} (nm)	D_{DLS} (nm)	PDI
MB-1	300	45	147	437	0.084
MB-2	287	58	164	503	0.068
MB-3	276	69	228	572	0.026
MB-4	265	80	285	620	0.093

[a]In the recipe, the weight of initiator AIBN is 6.9 mg; The solvent amount of acetonitrile is 20 mL; The reaction time is 0.5 h.

around 0.1, which meant that the nanohydrogels were very uniform. Besides, the spherical morphology and uniform size were also confirmed by TEM in Figure 1A. A possible reason

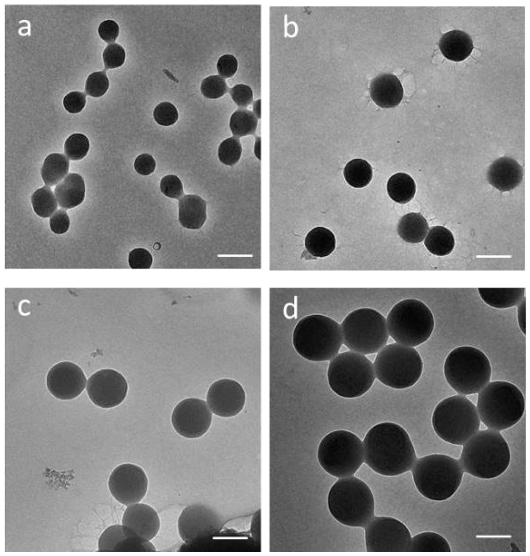

Figure 1. Representative TEM images of PMAA nanohydrogels with different cross-linker amounts: (a) MB-1, (b) MB-2, (c) MB-3, (d) MB-4. All scale bars are 200 nm.

accounting for the change of particle size is the high reaction activity of the cross-linker, which increased the number of the primary nuclei in the early stage and promoted the primary nuclei aggregate to form the large nanohydrogels.

The FTIR spectra in Figure 2A displayed the typical amide I (1650 cm^{-1}) and amide II (1550 cm^{-1}) bands of BACy cross-linker, suggesting the existence of disulfide cross-linker in the nanohydrogels. As the cross-linker amount increased from 15, 20, 25, to 30 wt %, the intensity of amide bands of BACy became stronger and stronger. Considering the factors of size, yield and cross-linking degree comprehensively, we chose sample MB-1 for the further investigation.

3.2. Preparation and Characterization of (FA&PEG)-Conjugated PMAA Nanohydrogels. After the preparation of the nanohydrogels, they were modified with folic acid to endow them with the ability of active targeting, and with PEG for obtaining the long in vivo circulation lifetime. FA has the characterized peaks of benzene framework at 1612 and 1508 cm^{-1}. In FITR spectra (Figure 2B), the pure PMAA nanohydrogels (MB-1) show obvious typical amide I (1647 cm^{-1}) and amide II (1536 cm^{-1}) bands of BACy cross-linker. After modification [(FA&PEG)-MB-1], the overlaid absorption of benzene framework and amide bond showed the blue-shifted and strengthened peaks at 1661 and 1543 cm^{-1}, which verified the success modification of FA. Besides, the C−O stretching vibration of the ether bond in PEG (1014 cm^{-1}) was found in the spectra, suggesting that PEG were also successfully grafted onto the surface of the nanohydrogels. The UV−vis spectra further confirmed the successful reaction for each step (Figure S1), FA-NH_2 molecule has strong absorbance at 282 nm, whereas the pure PMAA nanohydrogel has not. Compared with the UV−vis spectra before and after reaction with aminated FA, we can ensure the successful modification of FA on the surface of PMMA nanohydrogels.

Compared with the PMAA nanohydrogels (Sample MB-1), the TEM image of FA- and PEG-modified nanohydrogels (Sample (FA&PEG)-MB-1) still maintained the spherical and uniform structure (Figure S2). The DLS data (Table 2) demonstrated that the Z-average size mainly remained unchanged after FA-NH_2 molecule conjugation, whereas the

Table 2. Characterization Data of the Nanohydrogels after Modification with FA and PEG

sample code	D_{DLS}/nm	PDI	zeta potential (mV)
MB-1	437	0.084	−30.8
FA-MB-1	403	0.075	−34.8
PEG-MB-1	556	0.126	−20.5
(FA&PEG)-MB-1	551	0.147	−27.1

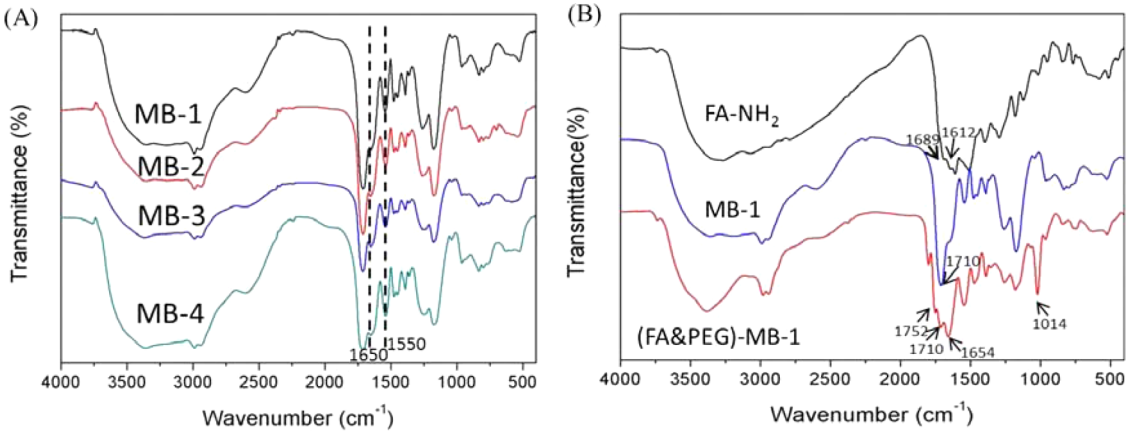

Figure 2. FTIR spectra of (A) PMAA nanohydrogels with different cross-linking degrees (MB-1 to MB-4); (B) nanohydrogels before and after modification with FA and PEG.

DOI: 10.1021/acsami.5b05984
ACS Appl. Mater. Interfaces 2015, 7, 19843−19852

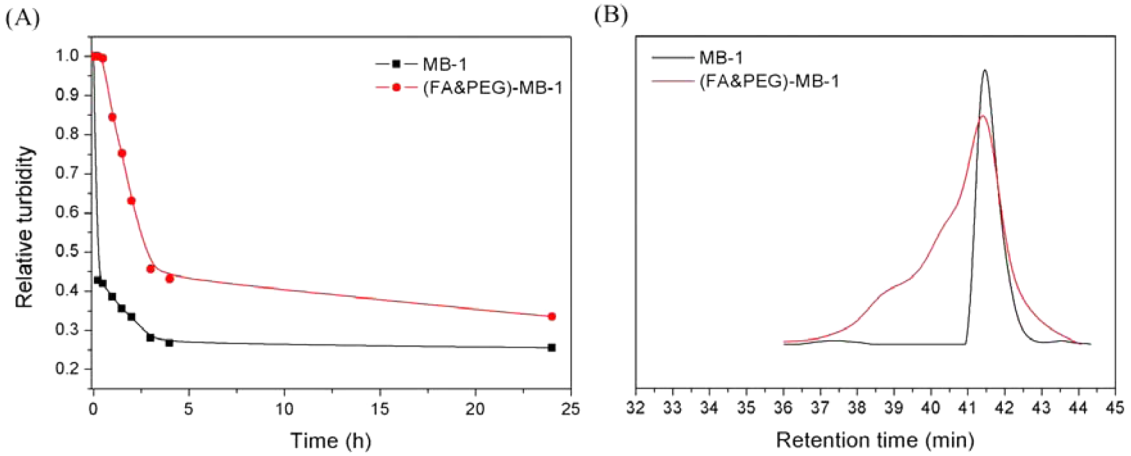

Figure 3. (A) Investigations on the redox-induced degradation of sample MB-1 and (FA&PEG)-MB-1 nanohydrogels by turbidity measurements; (B) GPC curves of sample MB-1 and (FA&PEG)-MB-1 after degradation for 24 h by 10 mM GSH.

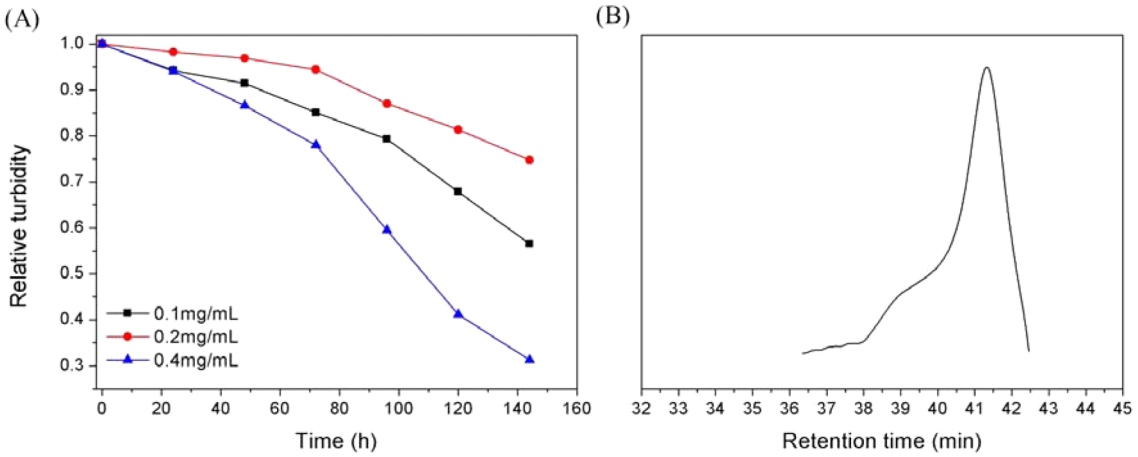

Figure 4. (A) Investigations on the protease-mediated degradation of sample (FA&PEG)-MB-1 nanohydrogels under different concentrations of protease by turbidity measurements; (B) GPC curve of sample (FA&PEG)-MB-1 after degradation by protease.

zeta potential became more negative because of the electronegative carboxyl groups in FA molecule. However, after PEG modification, the DLS data showed that the Z-average size of the nanohydrogels increased by about 150 nm, and the better colloidal dispersibility of the PEGlated nanohydrogels in water suggested the well stretching of ductile hydrophilic segments of PEG conjugated to the surface of nanohydrogels. Because the amino of PEG neutralized the carboxyl of MAA, the zeta potential of the as-prepared nanohydrogels became less negative, which would benefit the long circulation of the nanodrugs.

3.3. Reduction-Triggered Degradation of the (FA&PEG)-PMAA Nanohydrogels. The disulfide bond in the cross-linker BACy can be broken by the reductant GSH and lead to the degradation of the nanohydrogels in tumor cells. In this part, the degradation behavior of nanohydrogels was studied by the turbidity measurement (Figure 3A). Upon the addition of water-soluble GSH as a reducing agent, the skeleton network of the nanohydrogels was quickly degraded into individual short polymer chains, and the appearance of the milky emulsion changed gradually to a clear solution, whereas the structure of the nanohydrogels was very robust in the solution without GSH. For (FA&PEG)-PMAA nanohydrogels, the time of degradation progress became longer than that of sample MB-1 due to the existence of PEG segments on the surface, which will hinder GSH from entering the skeleton network to contact and react with disulfide bonds.

The molecular weights of the degraded sample MB-1 and (FA&PEG)-MB-1 nanohydrogels were measured by GPC (Figure 3B). The GPC results indicated the (FA&PEG)-MB-1 nanohydrogels were degraded into very small polymer chains with low molecular weight (M_n = 1121) and relative narrow molecular weight distribution (M_w/M_n = 1.34). The molecular weight became larger and the molecular weight distribution became wider compared with MB-1 nanohydrogels (M_n = 1070, M_w/M_n = 1.02), mainly because of the PEG conjugated to part of PMAA molecular chains.

3.4. Protease-Mediated Degradation of the (FA&PEG)-PMAA Nanohydrogels. Becuse of the amido bonds existing in the cross-linker BACy, similar to the structure of protein, an assumption was made that the nanohydrogels could be degraded by protease. To verify this speculation, we adopted protease K to conduct the degradation experiments, it is a serine protease that cleaves peptide bonds adjacent to the carboxylic group of aliphatic and aromatic amino acids, and the degradation behavior of nanohydrogels was studied by the turbidity measurement (Figure 4A). After addition of protease K, the turbidity of system decreased gradually, indicating the breaking of the skeleton network into short polymer chains. The degradation speed obviously enhanced as the concen-

DOI: 10.1021/acsami.5b05984
ACS Appl. Mater. Interfaces 2015, 7, 19843−19852

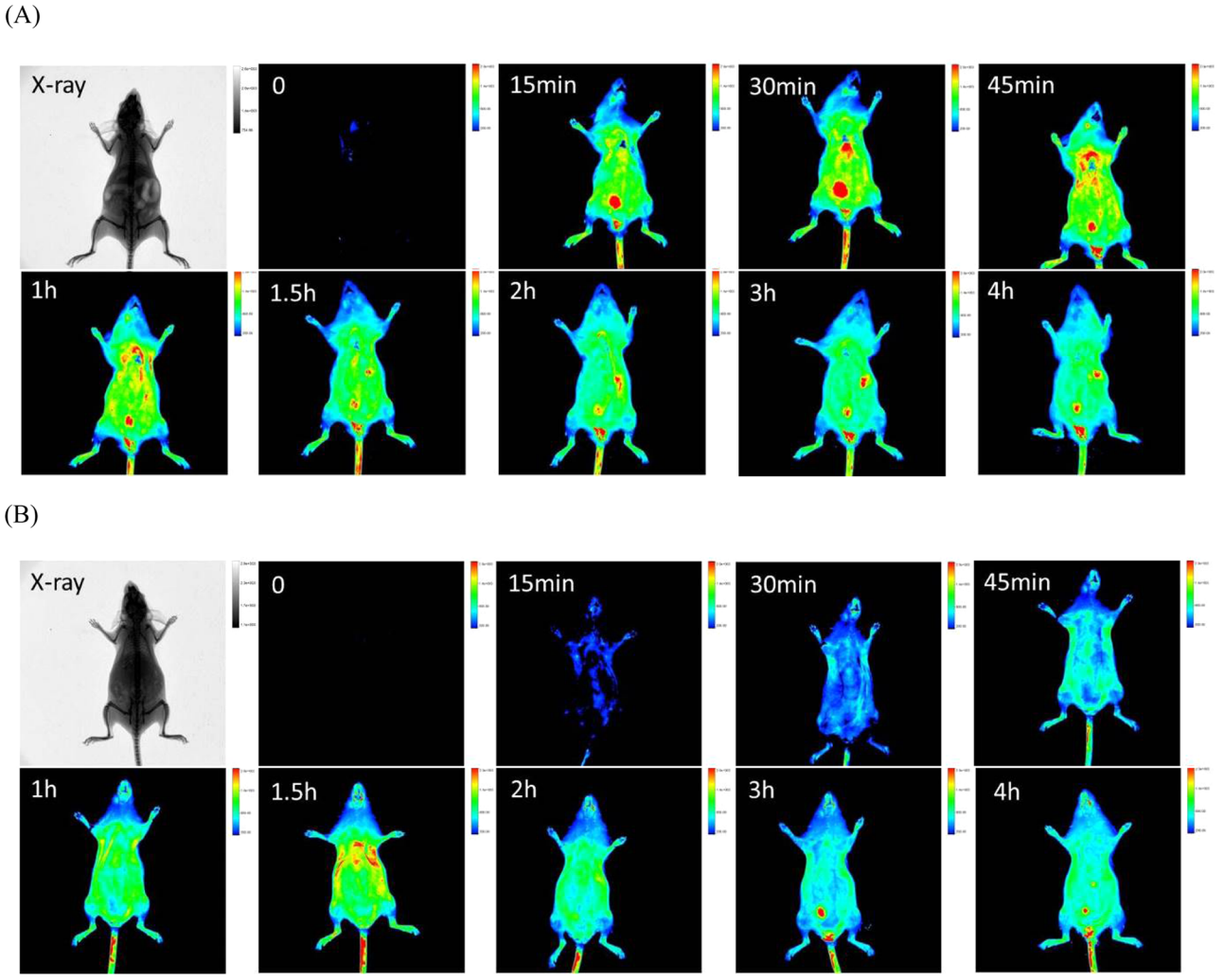

Figure 5. Intravital real-time fluorescence images of ICR mice injected with FITC-labeled PMAA nanohydrogels (A) before and (B) after PEG modification at different time scales.

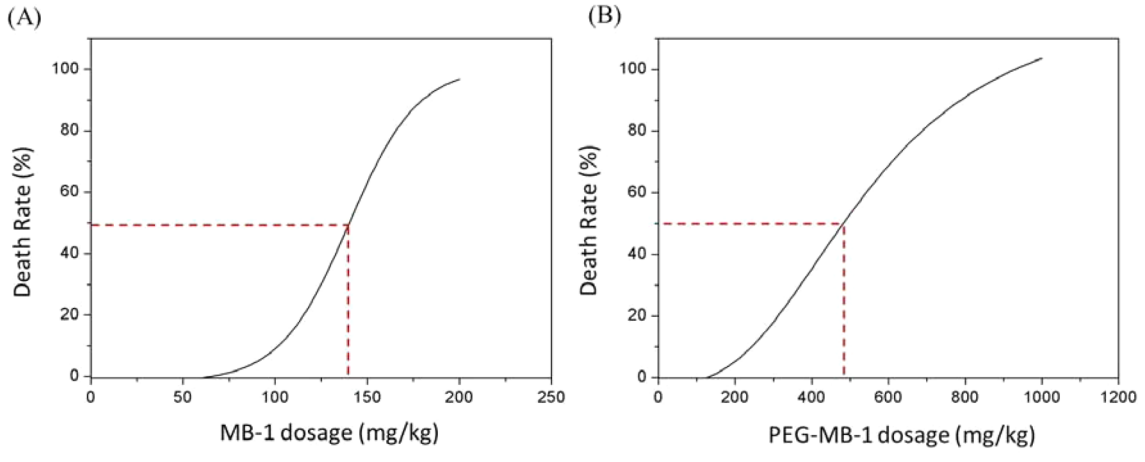

Figure 6. Acute toxicity curves of pure PMAA nanohydrogels (A) before and (B) after PEG modification.

tration of protease K increased from 0.1 to 0.3 mg/mL. Complete degradation was reached after 7 days for the quickest one. The GPC results (Figure 4B) showed that the nanohydrogels were degraded into small polymer chains with low molecular weight (M_n = 1176) and relative narrow molecular weight distribution (M_w/M_n = 1.27). This result implied that the nanohydrogels could be degraded in normal cells and tissues, and the formed short polymer chains could be metabolized through kidney eventually.

3.5. In Vivo Assessment of the Circulation Lifetime and Acute Toxicity. It is widely accepted that PEG can create a hydrophilic protective layer around the nanomaterials, which

DOI: 10.1021/acsami.5b05984
ACS Appl. Mater. Interfaces 2015, 7, 19843−19852

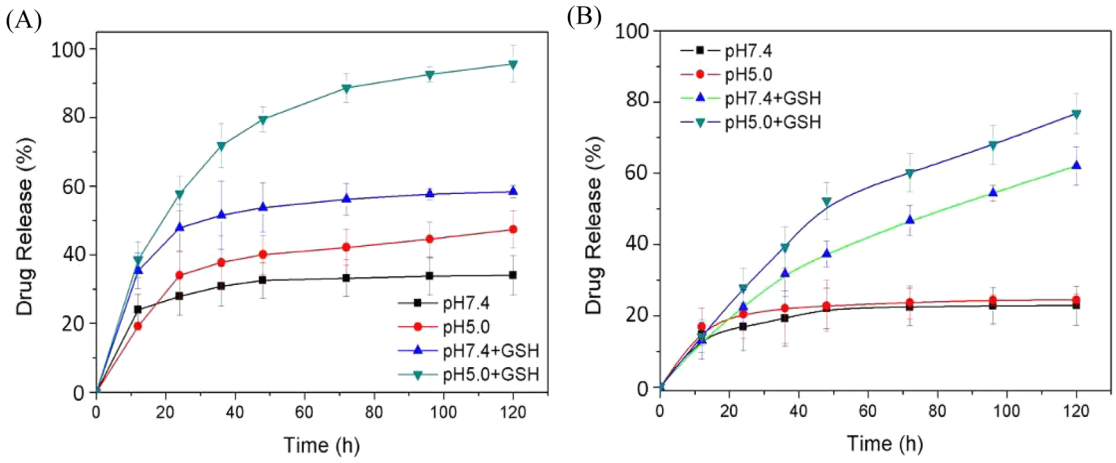

Figure 7. Redox and pH dual-responsive drug release profiles from the dual-drug-loaded (FA&PEG)-MB-1 nanohydrogels of (A) DOX and (B) PTX.

sterically hinders the adsorption of opsonin proteins, thereby blocking the opsonization process.[43] Thus, PEG-modified nanomaterials can be "hidden" from clearance and immune system to prolong blood circulation time in vivo. The intravital real-time fluorescence imaging analysis (Figure 5A) indicated that the FITC-labeled PMAA nanohydrogels were quickly gathered and stayed in the kidney after caudal vein injection of 15 min because of the high density of the surface charges, and the fluorescence intensity of the kidney is very strong. After 30 min, more and more FITC-labeled nanohydrogels accumulated in the kidney and liver, and the fluorescence intensity reached peak value. Meanwhile, the nanohydrogels also reached and gathered in other organs like the heart, lung, and spleen following blood circulation. After that, the fluorescence intensity decreased gradually in kidney and liver and faded away in other organs as well. However, for the PEGlated FITC-labeled PMAA nanohydrogels, the nanohydrogels spread homogeneously all over the body in the first 2 h (Figure 5B), and then part of the nanohydrogels gathered in kidney after 3 h, no obvious accumulation was observed in liver. The fluorescence intensity in kidney at 3h is also lower compared with the maximum fluorescence intensity of non-PEGlated nanohydrogels at 30 min. These results meant that the PEGlated FITC-labeled PMAA nanohydrogels had longer in vivo circulation lifetime than that of the non-PEGlated one, which is very important for the targeting drug delivery.

The acute toxicity studies for PMAA nanohydrogels were carried out to evaluate the toxicity of these materials in vivo. The dispersed suspension of non-PEGlated and PEGlated PMAA nanohydrogels were injected through caudal vein at grade doses, respectively. The lethality was observed for each dose and the acute toxicity curves (Figure 6) were recorded according to the relationship between dose and lethality. The classic measure of toxicity, lethal dose (LD_{50}, the dose at which mortality occurs in 50% of the study population) could be calculated from the fitted curve. The LD_{50} for PMAA nanohydrogels was 138.4 mg/kg, whereas that for PEGlated PMAA nanohydrogels was 499.7 mg/kg, which meant that the biological tolerance for the nanohydrogels increased tremendously through PEGylation.

3.6. Drugs Loading and in Vitro Release Kinetics of the (FA&PEG)-PMAA Nanohydrogels. Both relative high PTX loading capacity (DLC = 17.2 wt %) and drug loading efficiency (DLE = 92.5%) could be obtained owing to the strong interaction between the hydrophobic microdomain of disulfide bonds and PTX. Meanwhile, DOX was easily loaded in the (FA&PEG)-PMAA nanohydrogels with high DLC (23.3%) and DLE (98.8%) simultaneously because the carboxyl group has strong electrostatic interaction with the amino group. As the control experiments, we also prepared the samples of (FA&PEG)-PMAA nanohydrogels merely loading DOX and PEG−PMAA nanohydrogels loading both DOX and PTX with similar loading amount.

Accounting for the varying pH and redox potential between the extracellular and intracellular environments of tumor cells, the drug release experiment was designed and conducted by subjecting to different buffer solutions with pH values of 7.4 and 5.0 and whether adding GSH or not. As shown in Figure 7A, the amount of released DOX is only 30% at pH 7.4 without GSH over a period time of 48 h. When adding 10 mM GSH (mimicking the intracellular environment with GSH concentration about 2−10 mM), it showed a quick drug release, where the DOX cumulative release was approximately 57 wt % after 48 h. Under acidic pH conditions (pH 5.0), the DOX drug release was faster than that in the physiological solution, indicating the sensitivity of the drug-loaded (FA&PEG)-PMAA nanohydrogels to the endo/lysosomal pH. In the absence of GSH, DOX released from the carriers at pH 5.0 was about 48 wt % after 48 h. In the presence of 10 mM GSH at pH 5.0, the DOX release was closed to 80 wt % within the initial 48 h and reached to 98% ultimately, indicating its excellent dual-stimuli response property. All the DOX release curves approached nearly flattening after 48 h. Similar stimuli-responsive discipline was found for PTX release (Figure 7B), but the release continued for GSH added samples after 48h with a steady speed. Apparently, the release of PTX is an andante course of events compared with the quick release of DOX, which could produce subsequent killing for the remaining cells survived from first-round attack to solve the problem of tumor cell tolerance for one drug.

3.7. In Vitro Cell Assays. To further demonstrate whether the (FA&PEG)-MB-1 nanohydrogels can be efficiently internalized by cancer cells, we incubated the dual-drug-loaded (FA&PEG)-MB-1 nanohydrogels with HeLa cells for 24 h at 37 °C, and the cellular distribution was evaluated by confocal laser scanning microscopy (CLSM) analysis at the time scale of 2, 6, and 24 h. As shown in Figure 8, after 2 h incubation, the red fluorescence was observed in both the cytoplasm and the cell

DOI: 10.1021/acsami.5b05984
ACS Appl. Mater. Interfaces 2015, 7, 19843−19852

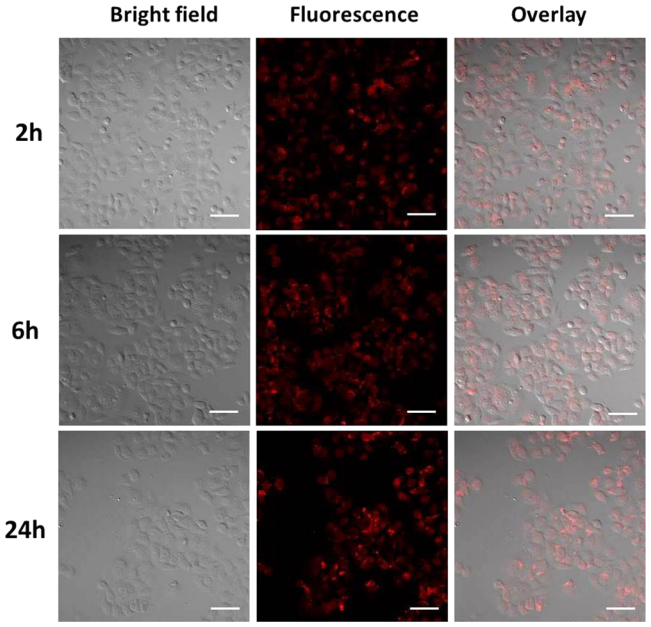

Figure 8. CLSM images of HeLa cells after 2, 6, and 24 h incubation with dual-drug-loaded (FA&PEG)-MB-1 nanohydrogels. The images showed bright-field, DOX fluorescence in cells (red), and overlays of the first two images. All scale bars are 1 μm.

nucleus, indicating that DOX molecules were released from drug-loaded (FA&PEG)-MB-1 nanohydrogels to the cytoplasm and entered into the cell nucleus subsequently. As time went on, the enhanced intensity of red fluorescence reflected that more DOX had been released because of the lower pH and the degradation of the disulfide-crossed nanohydrogels. The free DOX in cell nucleus could insert DNA to cause the cellular death, which should be attributed to the efficient intracellular delivery and release of DOX by (FA&PEG)-MB-1 carriers.

After that, standard CCK-8 assay was adopted to assess the cytotoxicity of pure (FA&PEG)-MB-1, drug-loaded (FA&PEG)-MB-1 nanohydrogels and free drugs at different concentrations. The experimental data (Figure S3) showed that, after incubation with the normal cells (HEK 293T) for 24h and 48h in a wide range of the concentrations (5−1000 μg/mL) of (FA&PEG)-MB-1, no obvious cytotoxicity could be detected even at relatively high concentrations. As for drug-loaded nanohydrogels (Figure 9), the DOX-loaded (FA&PEG)-MB-1 nanohydrogels indicated lower cytotoxicity to tumor cells (HeLa) compared to free DOX, while dual-drug-loaded (FA&PEG)-MB-1 nanohydrogels showed much better effect for killing tumor cells in contrast with the corresponding free drugs. As we mentioned above, it is not easy for free PTX to be administrated in cancer therapy due to its hydrophobicity, so the biocompatible nanohydrogels as carrier can overcame the obstacle to deliver the PTX into tumor cells, which can achieve better synergistic effect with DOX. Compared the dual-drug-loaded (FA&PEG)-MB-1 nanohydrogels with dual-drug-loaded PEG-MB-1 nanohydrogels, the greater cytotoxicity of the FA-conjugated one demonstrated the excellent active targeting ability of the surface folate ligand. After 48 h, the disparity became more evident between the two kinds of nanohydrogels, the dual-drug-loaded (FA&PEG)-MB-1 sample existed outstanding targeting and lethality for HeLa cells.

CONCLUSION

A series of uniform biodegradable PMAA nanohydrogels was prepared through a facile reflex-precipitation polymerization, the disulfide bond in the cross-linker BACy and carboxyl group in PMAA chain endowed the nanohydrogels with redox/pH dual stimuli-responsive ability, which guaranteed the quick release of drugs in the tumor cells. Besides, the nanohydrogels could be biodegraded into short polymer chains through cutting off the amido bonds by protease, which enhanced their metabolism in the whole human body. The in vitro and in vivo experiments showed that the dual-drug-loaded (FA&PEG)-MB-1 nanohydrogels possessed favorable targeting ability and therapeutic effects. Moreover, the acute toxicity assessment and intravital fluorescence imaging experiments demonstrated that the (FA&PEG)-MB-1 nanohydrogels possessed lower biotoxicity and longer in vivo blood circulation lifetime. All these results hint that the PEGlated multifunctional nanohydrogels have great potential as drug carrier for cancer therapy.

ASSOCIATED CONTENT

Supporting Information

The Supporting Information is available free of charge on the ACS Publications website at DOI: 10.1021/acsami.5b05984.

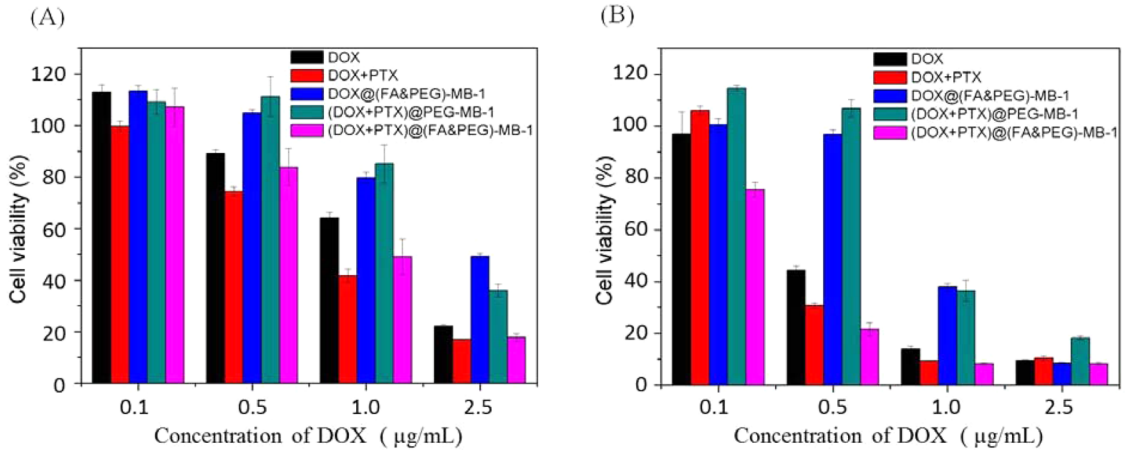

Figure 9. Cell viability of drug-loaded (FA&PEG)-MB-1 nanohydrogels and free drugs as a function of DOX dosages for (A) 24 h and (B) 48 h incubation with HeLa cells.

DOI: 10.1021/acsami.5b05984
ACS Appl. Mater. Interfaces 2015, 7, 19843−19852

UV−vis spectra of PMAA nanohydrogels before and after modification with FA and PEG; TEM image of PMAA nanohydrogels after modification with FA and PEG; in vitro cell viability of HEK 293T cells incubated with pure (FA&PEG)-MB-1 at different concentrations for 24 and 48 h (PDF)

AUTHOR INFORMATION

Corresponding Author

*E-mail: ccwang@fudan.edu.cn.

Notes

The authors declare no competing financial interest.

ACKNOWLEDGMENTS

This work was supported by National Science and Technology Key Project of China 2012AA020204), National Science Foundation of China (Grant 21474017), and Science and Technology Commission of Shanghai (Grant 13JC1400500)

REFERENCES

(1) Malachowski, K.; Breger, J.; Kwag, H. R.; Wang, M. O.; Fisher, J. P.; Selaru, F. M.; Gracias, D. H. Stimuli-Responsive Theragrippers for Chemomechanical Controlled Release. *Angew. Chem., Int. Ed.* **2014**, *53*, 8045−8049.

(2) Basit, A. W. Advances in Colonic Drug Delivery. *Drugs* **2005**, *65*, 1991−2007.

(3) Zhang, L.; Wang, Y.; Yang, Y. T.; Liu, Y. Y.; Ruan, S. B.; Zhang, Q. Y.; Tai, X. W.; Chen, J. T.; Xia, T.; Qiu, Y.; Gao, H. L.; He, Q. High Tumor Penetration of Paclitaxel Loaded pH Sensitive Cleavable Liposomes by Depletion of Tumor Collagen I in Breast Cancer. *ACS Appl. Mater. Interfaces* **2015**, *7*, 9691−9701.

(4) Patra, S.; Roy, E.; Karfa, P.; Kumar, P.; Madhuri, R.; Sharma, P. K. Dual-Responsive Polymer Coated Superparamagnetic Nanoparticle for Targeted Drug Delivery and Hyperthermia Treatment. *ACS Appl. Mater. Interfaces* **2015**, *7*, 9235−9246.

(5) Oh, J. K.; Drumright, R.; Siegwart, D. G.; Matyjaszewski, K. The Development of Microgels/Nanogels for Drug Delivery Applications. *Prog. Polym. Sci.* **2008**, *33*, 448−477.

(6) Kabanov, A. V.; Vinogradov, S. V. Nanogels as Pharmaceutical Carriers: Finite Networks of Infinite Capabilities. *Angew. Chem., Int. Ed.* **2009**, *48*, 5418−5429.

(7) Ghosh, R.; Goswami, U.; Ghosh, S. S.; Paul, A.; Chattopadhyay, A. Synergistic Anticancer Activity of Fluorescent Copper Nanoclusters and Cisplatin Delivered through a Hydrogel Nanocarrier. *ACS Appl. Mater. Interfaces* **2015**, *7*, 209−222.

(8) Pan, Y. J.; Li, D.; Jin, S.; Wei, C.; Wu, K. Y.; Guo, J.; Wang, C. C. Folate-conjugated poly(N-(2-hydroxypropyl)methacrylamide-co-methacrylic acid) nanohydrogels with pH/redox dual-stimuli response for controlled drug release. *Polym. Chem.* **2013**, *4*, 3545−3553.

(9) Drummond, D. C.; Meyer, O.; Hong, K.; Kirpotin, D. B.; Papahadjopoulos, D. Optimizing Liposomes for Delivery of Chemotherapeutic Agents to Solid Tumors. *Pharmacol. Rev.* **1999**, *51*, 691−743.

(10) Molineux, G. PEGylation: Engineering Improved Pharmaceuticals for Enhanced Therapy. *Cancer Treat. Rev.* **2002**, *28*, 13−16.

(11) Chiang, Y. T.; Lo, C. L. Ph-Responsive Polymer-Liposomes for Intracellular Drug Delivery and Tumor Extracellular Matrix Switched-On Targeted Cancer Therapy. *Biomaterials* **2014**, *35*, 5414−5424.

(12) Allen, T. M. Ligand-Targeted Therapeutics in Anticancer Therapy. *Nat. Rev. Cancer* **2002**, *2*, 750−763.

(13) Lu, Y.; Low, P. S. Folate-Mediated Delivery of Macromolecular Anticancer Therapeutic Agents. *Adv. Drug Delivery Rev.* **2012**, *64*, 342−352.

(14) Mornet, E.; Carmoy, N.; Lainé, C.; Lemiègre, L.; Le Gall, T.; Laurent, I.; Marianowski, R.; Férec, C.; Lehn, P.; Benvegnu, T.; Montier, T. Folate Equipped Nanolipoplexes Mediated Efficient Gene Transfer into Humanepithelial Cells. *Int. J. Mol. Sci.* **2013**, *14*, 1477−1501.

(15) Li, L.; Yang, Q. Q.; Zhou, Z.; Zhong, J. J.; Huang, Y. Doxorubicin-Loaded, Charge Reversible, Folate Modified HPMA Copolymer Conjugates for Active Cancer Cell Targeting. *Biomaterials* **2014**, *35*, 5171−5187.

(16) Wang, C.; Wang, Y.; Wang, Y.; Fan, M.; Luo, F.; Qian, Z. Y. Characterization, Pharmacokinetics and Disposition of Novel Nano-scale Preparations of Paclitaxel. *Int. J. Pharm.* **2011**, *414*, 251−259.

(17) Peng, J. R.; Qi, T. T.; Liao, J. F.; Chu, B. Y.; Yang, Q.; Li, W. Y.; Qu, Y.; Luo, F.; Qian, Z. Y. Controlled Release of Cisplatin from pH-Thermal Dual Responsive Nanogels. *Biomaterials* **2013**, *34*, 8726−8740.

(18) Chen, Y.; Zheng, X.; Qian, H.; Mao, Z.; Ding, D.; Jiang, X. Hollow Core-Porous Shell Structure Poly(Acrylic Acid) Nanogels with a Superhigh Capacity of Drug Loading. *ACS Appl. Mater. Interfaces* **2010**, *2*, 3532−3538.

(19) Akiyoshi, K.; Kobayashi, S.; Shichibe, S.; Mix, D.; Baudys, M.; Kim, S. W.; Sunamoto, S. Self-Assembled Hydrogel Nanoparticle of Cholesterol-Bearing Pullulan as a Carrier of Protein Drugs: Complexation and Stabilization of Insulin. *J. Controlled Release* **1998**, *54*, 313−320.

(20) Tamura, A.; Oishi, M.; Nagasaki, Y. Enhanced Cytoplasmic Delivery of siRNA Using a Stabilized Polyion Complex Based on PEGylated Nanogels with a Cross-Linked Polyamine Structure. *Biomacromolecules* **2009**, *10*, 1818−1827.

(21) Chen, G. J.; Wang, L. W.; Cordie, T.; Vokoun, C.; Eliceiri, K. W.; Gong, S. Q. Multi-Functional Self-Fluorescent Unimolecular Micelles for Tumor-Targeted Drug Delivery and Bioimaging. *Biomaterials* **2015**, *47*, 41−50.

(22) Lehár, J.; Krueger, A. S.; Avery, W.; Heilbut, A. M.; Johansen, L. M.; Price, E. R.; Rickles, R. J.; Short, G. F.; Staunton, J. E.; Jin, X.; Lee, M. S.; Zimmermann, G. R.; Borisy, A. A. Synergistic Drug Combinations Tend to Improve Therapeutically Relevant Selectivity. *Nat. Biotechnol.* **2009**, *27*, 659−666.

(23) Bahadur, K. C. R.; Xu, P. S. Multicompartment Intracellular Self-Expanding Nanogel for Targeted Delivery of Drug Cocktail. *Adv. Mater.* **2012**, *24*, 6479−6483.

(24) Liechty, W. B.; Scheuerle, R. L.; Peppas, N. A. Tunable, Responsive Nanogels Containing t-Butyl Methacrylate and 2-(t-Butylamino) Ethyl Methacrylate. *Polymer* **2013**, *54*, 3784−3795.

(25) Fang, J.; Nakamura, H.; Maeda, H. The EPR Effect: Unique Features of Tumor Blood Vessels for Drug Delivery, Factors Involved, and Limitations and Augmentation of the Effect. *Adv. Drug Delivery Rev.* **2011**, *63*, 136−151.

(26) Han, N.; Zhao, Q. F.; Wan, L.; Wang, Y.; Gao, Y. K.; Wang, P.; Wang, Z. Y.; Zhang, J. H.; Jiang, T. Y.; Wang, S. L. Hybrid Lipid-Capped Mesoporous Silica for Stimuli-Responsive Drug Release and Overcoming Multidrug Resistance. *ACS Appl. Mater. Interfaces* **2015**, *7*, 3342−3351.

(27) Yu, A.; Shabahang, S.; Timiryasova, T. M.; Zhang, Q.; Beltz, R.; Gentschev, I.; Goebel, W.; Szalay, A. A. Visualization of Tumors and Metastases in Live Animals with Bacteria and Vaccinia Virus Encoding Light-Emitting Proteins. *Nat. Biotechnol.* **2004**, *22*, 313−320.

(28) Xiong, M. H.; Bao, Y.; Du, X. J.; Tan, Z. B.; Jiang, Q.; Wang, H. X.; Zhu, Y. H.; Wang, J. Differential Anticancer Drug Delivery With a Nanogel Sensitive to Bacteria-Accumulated Tumor Artificial Environment. *ACS Nano* **2013**, *7*, 10636−10645.

(29) Das, M.; Mardyani, S.; Chan, W. C. W.; Kumacheva, E. Biofunctionalized pH-Responsive Microgels for Cancer Cell Targeting: Rational Design. *Adv. Mater.* **2006**, *18*, 80−83.

(30) Duan, C. X.; Gao, J.; Zhang, D. R.; Jia, L. J.; Liu, Y.; Zheng, D. D.; Liu, G. P.; Tian, X. N.; Wang, F. S.; Zhang, Q. Galactose-Decorated pH-Responsive Nanogels for Hepatoma-Targeted Delivery of Oridonin. *Biomacromolecules* **2011**, *12*, 4335−4343.

(31) Chiang, W. H.; Ho, V. T.; Chen, H. H.; Huang, W. C.; Huang, Y. F.; Lin, S. C.; Chern, C. S.; Chiu, H. C. Superparamagnetic Hollow Hybrid Nanogels as a Potential Guidable Vehicle System of Stimuli-

DOI: 10.1021/acsami.5b05984
ACS Appl. Mater. Interfaces 2015, 7, 19843−19852

Mediated MR Imaging and Multiple Cancer Therapeutics. *Langmuir* **2013**, *29*, 6434−6443.
(32) Nel, A. E.; Madler, L.; Velegol, D.; Xia, T.; Hoek, E. M. V.; Somasundaran, P.; Klaessig, F.; Castranova, V.; Thompson, M. Understanding Biophysicochemical Interactions at the Nano-Bio Interface. *Nat. Mater.* **2009**, *8*, 543−557.
(33) Zhang, X. J.; Achazi, K.; Steinhilber, D.; Kratz, F.; Dernedde, J.; Haag, R. A Facile Approach for Dual-Responsive Prodrug Nanogels Based on Dendritic Polyglycerols with Minimal Leaching. *J. Controlled Release* **2014**, *174*, 209−216.
(34) Raemdonck, K.; Demeester, J.; De Smedt, S. Advanced Nanogel Engineering for Drug Delivery. *Soft Matter* **2009**, *5*, 707−715.
(35) Meng, F. H.; Hennink, W. E.; Zhong, Z. Y. Reduction-Sensitive Polymers and Bioconjugates for Biomedical Applications. *Biomaterials* **2009**, *30*, 2180−2198.
(36) Chen, W.; Zheng, M.; Meng, F. H.; Cheng, R.; Deng, C.; Feijen, J.; Zhong, Z. Y. In Situ Forming Reduction-Sensitive Degradable Nanogels for Facile Loading and Triggered Intracellular Release of Proteins. *Biomacromolecules* **2013**, *14*, 1214−1222.
(37) Jin, S.; Li, D.; Yang, P.; Guo, J.; Lu, J. Q.; Wang, C. C. Redox/pH Stimuli-Responsive Biodegradable PEGylated P(MAA/BACy) Nanohydrogels for Controlled Releasing of Anticancer Drugs. *Colloids Surf., A* **2015**, *484*, 47−55.
(38) Pan, Y. J.; Chen, Y. Y.; Wang, D. R.; Wei, C.; Guo, J.; Lu, D. R.; Chu, C. C.; Wang, C. C. Redox/pH Dual Stimuli-Responsive Biodegradable Nanohydrogels with Varying Responses to Dithiothreitol and Glutathione for Controlled Drug Release. *Biomaterials* **2012**, *33*, 6570−6579.
(39) Sun, Y. X.; Zeng, X.; Meng, Q. F.; Zhang, X. Z.; Cheng, S. X.; Zhuo, R. X. The Influence of RGD Addition on the Gene Transfer Characteristics of Disulfide-Containing Polyethyleneimine/DNA Complexes. *Biomaterials* **2008**, *29*, 4356−4365.
(40) Li, K.; Pan, J.; Feng, S. S.; Wu, A. W.; Pu, K. Y.; Liu, Y.; Liu, B. Generic Strategy of Preparing Fluorescent Conjugated-Polymer-Loaded Poly(DL-Lactide-co-Glycolide) Nanoparticles for Targeted Cell Imaging. *Adv. Funct. Mater.* **2009**, *19*, 3535−3542.
(41) Liong, M.; Lu, J.; Kovochich, M.; Xia, T.; Ruehm, S. G.; Nel, A. E.; Tamanoi, F.; Zink, J. I. Multifunctional Inorganic Nanoparticles for Imaging, Targeting, and Drug Delivery. *ACS Nano* **2008**, *2*, 889−896.
(42) Jin, S.; Pan, Y. J.; Wang, C. C. Reflux Precipitation Polymerization: A New Technology for Preparation of Monodisperse Polymer Nanohydrogels. *Huaxue Xuebao* **2013**, *71*, 1500−1504.
(43) Wang, B.; He, X.; Zhang, Z. Y.; Zhao, Y. L.; Feng, W. Y. Metabolism of Nanomaterials In Vivo: Blood Circulation and Organ Clearance. *Acc. Chem. Res.* **2013**, *46*, 761−769.

DOI: 10.1021/acsami.5b05984
ACS Appl. Mater. Interfaces 2015, 7, 19843−19852